



## NRC Publications Archive Archives des publications du CNRC

### **Prebiotic chemistry within a simple impacting icy mixture** Goldman, Nir; Tamblyn, Isaac

This publication could be one of several versions: author's original, accepted manuscript or the publisher's version. / La version de cette publication peut être l'une des suivantes : la version prépublication de l'auteur, la version acceptée du manuscrit ou la version de l'éditeur.

For the publisher's version, please access the DOI link below. / Pour consulter la version de l'éditeur, utilisez le lien DOI ci-dessous.

#### **Publisher's version / Version de l'éditeur:**

<https://doi.org/10.1021/jp402976n>

*The Journal of Physical Chemistry A*, 117, 24, pp. 5124-5131, 2013-05-02

#### **NRC Publications Record / Notice d'Archives des publications de CNRC:**

<https://nrc-publications.canada.ca/eng/view/object/?id=e89d2ac7-4cf8-40e0-bcc9-3c53f68ed70a>

<https://publications-cnrc.canada.ca/fra/voir/objet/?id=e89d2ac7-4cf8-40e0-bcc9-3c53f68ed70a>

Access and use of this website and the material on it are subject to the Terms and Conditions set forth at

<https://nrc-publications.canada.ca/eng/copyright>

READ THESE TERMS AND CONDITIONS CAREFULLY BEFORE USING THIS WEBSITE.

L'accès à ce site Web et l'utilisation de son contenu sont assujettis aux conditions présentées dans le site

<https://publications-cnrc.canada.ca/fra/droits>

LISEZ CES CONDITIONS ATTENTIVEMENT AVANT D'UTILISER CE SITE WEB.

**Questions?** Contact the NRC Publications Archive team at

PublicationsArchive-ArchivesPublications@nrc-cnrc.gc.ca. If you wish to email the authors directly, please see the first page of the publication for their contact information.

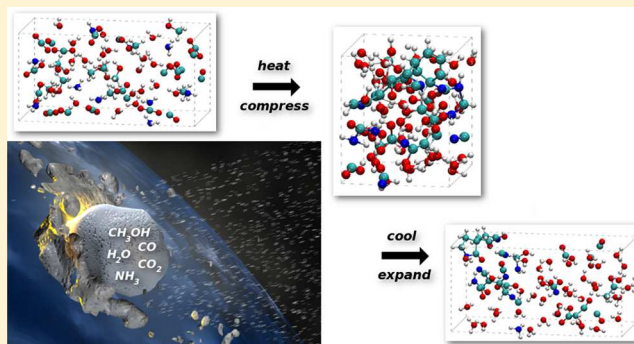
**Vous avez des questions?** Nous pouvons vous aider. Pour communiquer directement avec un auteur, consultez la première page de la revue dans laquelle son article a été publié afin de trouver ses coordonnées. Si vous n'arrivez pas à les repérer, communiquez avec nous à PublicationsArchive-ArchivesPublications@nrc-cnrc.gc.ca.



## Prebiotic Chemistry within a Simple Impacting Icy Mixture

Nir Goldman<sup>\*,†</sup> and Isaac Tamblyn<sup>‡</sup><sup>†</sup>Physical and Life Sciences Directorate, Lawrence Livermore National Laboratory, Livermore, California 94550, United States<sup>‡</sup>Department of Physics, University of Ontario Institute of Technology, Oshawa, ON L1H 7K4, Canada

**ABSTRACT:** We present results of prebiotic organic synthesis in shock compressed mixtures of simple ices from quantum molecular dynamics (MD) simulations extended to close to equilibrium time scales. Given the likelihood of an inhospitable prebiotic atmosphere on early Earth, it is possible that impact processes of comets or other icy bodies were a source of prebiotic chemical compounds on the primitive planet. We observe that moderate shock pressures and temperatures within a CO<sub>2</sub>-rich icy mixture (36 GPa and 2800 K) produce a number of nitrogen containing heterocycles, which dissociate to form functionalized aromatic hydrocarbons upon expansion and cooling to ambient conditions. In contrast, higher shock conditions (48–60 GPa, 3700–4800 K) resulted in the synthesis of long carbon-chain molecules, CH<sub>4</sub>, and formaldehyde. All shock compression simulations at these conditions have produced significant quantities of simple C–N bonded compounds such as HCN, HNC, and HNCO upon expansion and cooling to ambient conditions. Our results elucidate a mechanism for impact synthesis of prebiotic molecules at realistic impact conditions that is independent of external constraints such as the presence of a catalyst, illuminating UV radiation, or pre-existing conditions on a planet.



## ■ INTRODUCTION

How and when prebiotic organic material (e.g., amino acids, sugars, purines, pyrimidines, etc.) appeared on early Earth has been debated without resolution in the open literature for close to 60 years. Considerable effort has focused on synthesis from materials already in existence on the primitive planet. Seminal experiments<sup>1,2</sup> observed amino acid synthesis in a vaporized reducing (H<sub>2</sub> and CH<sub>4</sub> rich) mixture subjected to electrical discharges, simulating hypothetical conditions on the early Earth. The purines and pyrimidines that constitute DNA and RNA nucleobases (adenine, guanine, cytosine, thymine, and uracil) have all been synthesized from HCN and urea ((NH<sub>2</sub>)<sub>2</sub>CO), which are known products of these experiments.<sup>3</sup> Prebiotic organic material has been synthesized under geothermal conditions in the presence of H<sub>2</sub> (e.g., refs 4 and 5) and through irradiation of reduced forms of carbon with ultraviolet (UV) light.<sup>6,7</sup> However, the current viewpoint is that the composition of early Earth's atmosphere was more oxidizing,<sup>8</sup> consisting mainly of CO<sub>2</sub>, with significantly lesser amounts of N<sub>2</sub>, H<sub>2</sub>S, HCl, and water vapor.<sup>3</sup> Shock heating experiments<sup>9,10</sup> and calculations<sup>11</sup> on aqueous mixtures have found that synthesis of organic molecules necessary for amino acid production is unlikely in a CO<sub>2</sub>-rich environment.

The possibility exists that both prebiotic raw materials and energy may have been delivered to the Earth simultaneously by a cometary impact.<sup>12</sup> Cometary ices are predominantly water,<sup>13</sup> containing many small molecules important to prebiotic aqueous chemistry, e.g., NH<sub>3</sub>, CH<sub>3</sub>OH,<sup>14</sup> and an impact can provide an abundant supply of energy to drive chemical

reactivity. Recent analysis of dust samples from comet Wild 2 have observed the presence of glycine in the captured material.<sup>15</sup> Interplanetary dust particles accrete icy layers consisting of H<sub>2</sub>O, CO, CO<sub>2</sub>, CH<sub>3</sub>OH, and NH<sub>3</sub>, which can form amino acids upon exposure to UV radiation.<sup>16</sup> The flux of organic matter to Earth via comets and asteroids during periods of heavy bombardment may have been as high as 10<sup>13</sup> kg/yr, delivering up to several orders of magnitude greater mass of organics than what likely pre-existed on the planet.<sup>17</sup>

Given its relatively large size (e.g., median nucleus radius between 1.61 and 56 km<sup>18</sup>), a comet passing through Earth's atmosphere will be heated externally but will remain cool internally. Upon impact with the Earth's surface, the resulting shock wave will compress a small section of material on a time scale that is limited by the rise time of the shock wave (<10 ps).<sup>19–21</sup> A shock wave causes a reactive material to visit numerous thermodynamic states during the course of compression. Shock waves can create sudden, intense pressures and temperatures that could affect chemical pathways and reactions within a comet before interactions with the ambient planetary atmosphere can occur. An oblique collision where an extraterrestrial icy body impacts a planetary atmosphere with a glancing blow could generate thermodynamic conditions conducive to organic synthesis.<sup>17</sup> These processes could result in significant concentrations of organic species being delivered

Received: March 26, 2013

Revised: April 25, 2013

Published: May 2, 2013



to Earth from exogenous sources. Shock compression experiments have shown that a high percentage of aqueous amino acids survived relatively low pressure conditions (412–870 K and 5–21 GPa; 1 GPa = 10 kbar)<sup>17</sup> and that mixtures resembling carbonaceous chondrites can produce a variety of organic material at pressures of ~6 GPa.<sup>22</sup> Nonetheless, to date there have been few studies on the production of prebiotic molecules at both extreme temperatures and pressures (e.g., >1000 K and 20 GPa) that result from impact of a large icy body such as a comet.

Molecular dynamics (MD) simulations can provide an accurate description of the chemical reactivity with a shock compressed body,<sup>23–33</sup> which can greatly facilitate experimental design and interpretation. Our initial quantum simulations with density functional theory (DFT) on a CO<sub>2</sub>-rich aqueous mixture showed the possibility of formation of the prebiotic amino acid glycine due to shock compression corresponding to planetary impacts at oblique angles.<sup>34</sup> We computed low free energies of formation for amino acids at acidic conditions similar to the atmosphere and oceans on early Earth. Our results have since been confirmed by shock recovery experiments on a similar mixture and at a single impact velocity, where several linear and methylamino acids including glycine have been produced.<sup>35</sup> However, due to the extreme computational cost of performing DFT-MD, our simulations were limited to time scales of approximately 10–30 ps, where chemical reactivity was clearly still far from equilibrium. In addition, experiments so far have been designed to detect synthesized amino acids, exclusively. Further experimentation would greatly benefit from detailed knowledge of the types of prebiotic molecules in addition to amino acids that can occur as a function of different peak thermodynamic conditions and initial chemical composition of the astrophysical ice.

We have extended our work to close to equilibrium time scales by using the density functional tight binding (DFTB) semiempirical approach to conduct MD simulations of the same CO<sub>2</sub>-rich aqueous mixture as our previous study. DFTB is an approximate quantum simulation technique that allows for several orders of magnitude increase in computational efficiency while retaining most of the accuracy of standard DFT.<sup>36</sup> DFTB methods generally use a minimal atom-centered basis set (e.g., s and p orbitals for carbon, only) and an approximate Hamiltonian based on Kohn–Sham DFT.<sup>37</sup> DFTB has been shown to yield accurate results for organic energetic materials at conditions up to 200 GPa and 4000 K.<sup>28,33,38–41</sup> It thus has the potential to achieve time scales relevant to experiments while providing an accurate picture of chemical reactivity over the broad range of thermodynamic conditions achieved by impacting materials.

Here, we divide our simulations of impacts into three distinct regions: (I) shock compression due to impact with the planetary surface, (II) adiabatic (free) expansion due to the rarefaction wave passing through the icy material, and (III) cooling and equilibration due to heat transfer to materials extant on the planet. We then analyze the chemical reactivity in each region. We find that shock compression yields a number of exotic C–C and C–N bonded species that are highly reactive and have short lifetimes. Expansion and cooling yields the formation of complex organic prebiotic species such as aromatic compounds, as well simple precursors to amino acids, depending on the strength of the initial shock compression. Our results indicate that impacts from cometary ices could have yielded a wide variety of prebiotic organic material in addition

to amino acids on early Earth, regardless of the initial chemical conditions on the planet.

## COMPUTATIONAL METHODS

DFTB calculations with self-consistent charges (SCC) were driven by the LAMMPS molecular software simulation suite,<sup>42</sup>

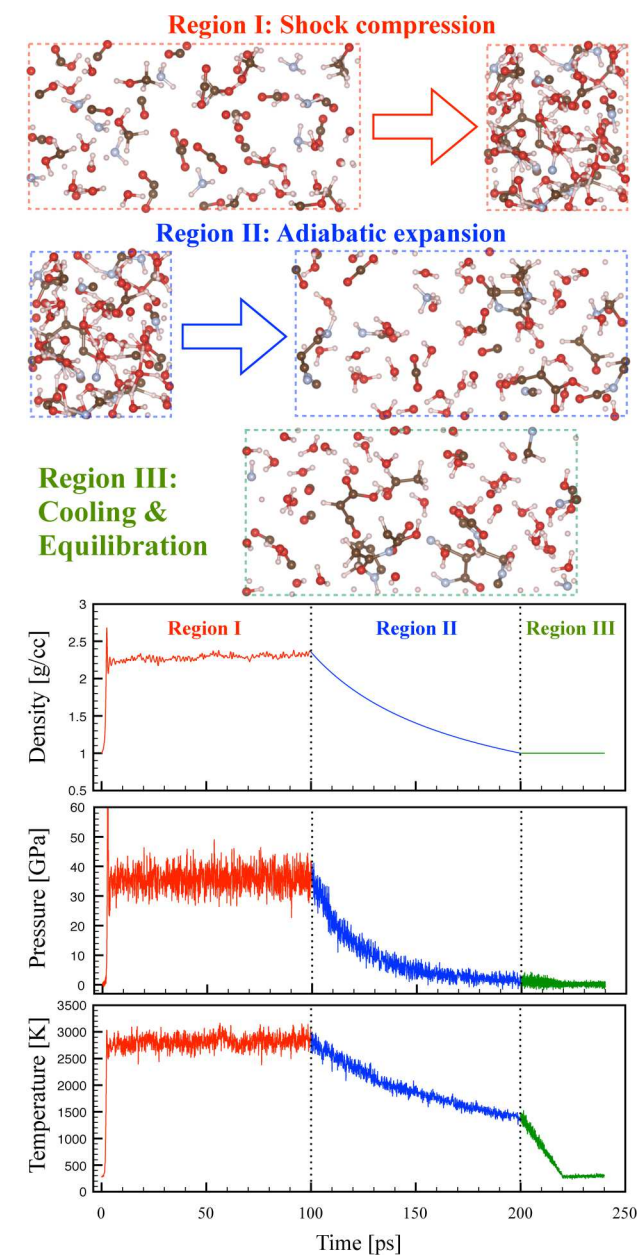


**Figure 1.** Thermodynamic conditions explored during (I) shock compression, (II) adiabatic expansion, and (III) final cooling and equilibration. Results above are for an initial shock pressure of  $P = 36$  GPa,  $T = 2800$  K. The thermodynamic conditions of the shock state vary depending on the impact velocity (or alternatively the angle of incidence).

with the DFTB+ code<sup>36</sup> used to compute forces and the cell stress tensor. We used C–H–O–N interaction parameters available for download (mio-0-1 parameter set from <http://www.dftb.org>). The maximum number of SCC steps for each MD time step was reduced to four through use of the Extended Lagrangian Born–Oppenheimer molecular dynamics (XL-

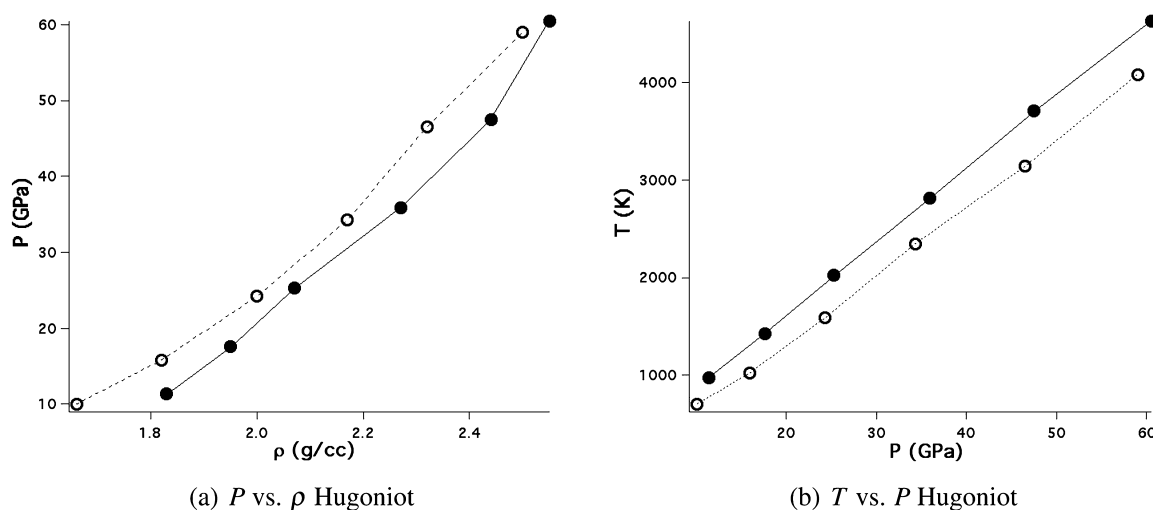


**Figure 2.** Comparison of Hugoniot curves. The open circles and dashed lines correspond to results from DFT, and the solid circles and lines to DFTB.

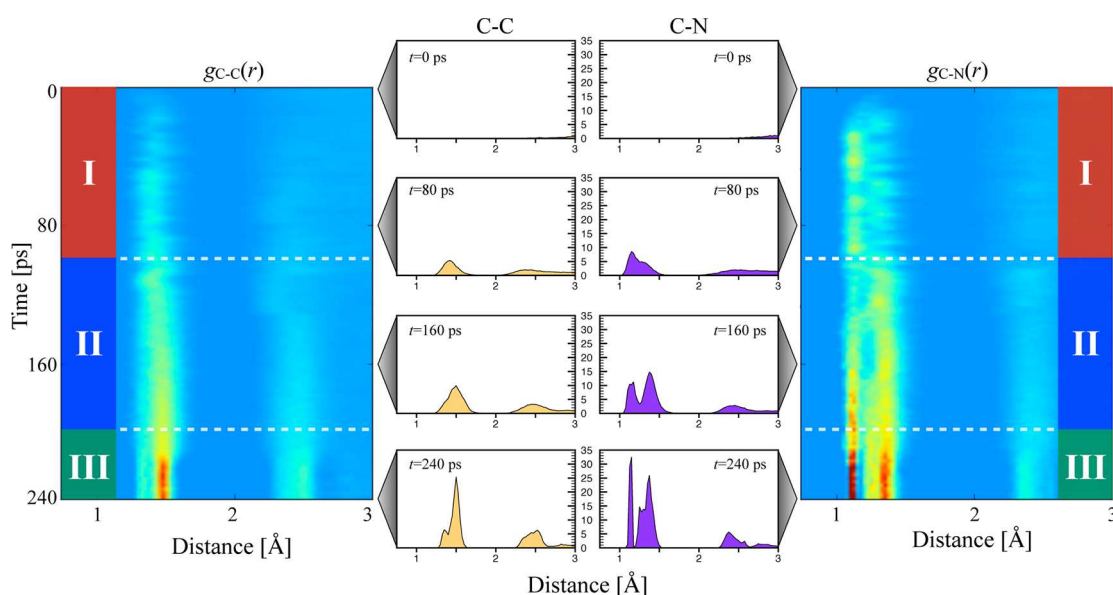


**Figure 3.** Time evolution of peak intensities of the C–C (left panel) and C–N (right panel) RDFs at shock conditions of 36 GPa and 2800 K. Line profiles of the RDFs at different points during the simulation are depicted in the middle panel. Initially, no C–C or C–N bonded species are present. During the initial 100 ps (region I), the system is in the shock state and C–C and C–N bonds are transient. In region II in this graphic, the system is expanded adiabatically at a fixed strain rate ( $100 \text{ ps}^{-1}$ ). We observe a quenching of chemical kinetics during the cooling phase of our simulations (region III).

BOMD) approach for propagation of the electronic degrees of freedom.<sup>43–48</sup> Thermal populations of excited electronic states are computed through the Mermin functional.<sup>49</sup> All simulations discussed here were performed with a time step of 0.2 fs. We used an initial astrophysical ice configuration of 20  $\text{H}_2\text{O}$ , 10  $\text{CH}_3\text{OH}$ , 10  $\text{NH}_3$ , 10  $\text{CO}$ , and 10  $\text{CO}_2$  molecules (210 atoms total), with computational-cell lattice vectors of  $a = 21.9150 \text{ \AA}$ ,  $b = 10.9575 \text{ \AA}$ , and  $c = 10.9575 \text{ \AA}$ , yielding a density of  $1.0 \text{ g/cm}^3$ . This yielded similar initial composition and density to experiments.<sup>16</sup> The initial icy mixture was equilibrated at 300 K for 20 ps using Nose–Hoover thermostat chains.<sup>50,51</sup> Uniaxial compression due to the shock wave and adiabatic expansion of the rarefaction wave occurred along the  $a$  lattice vector. Previous work has shown that doubling the system size along the  $a$  lattice vector yielded virtually identical thermodynamic conditions under shock loading.<sup>34</sup>

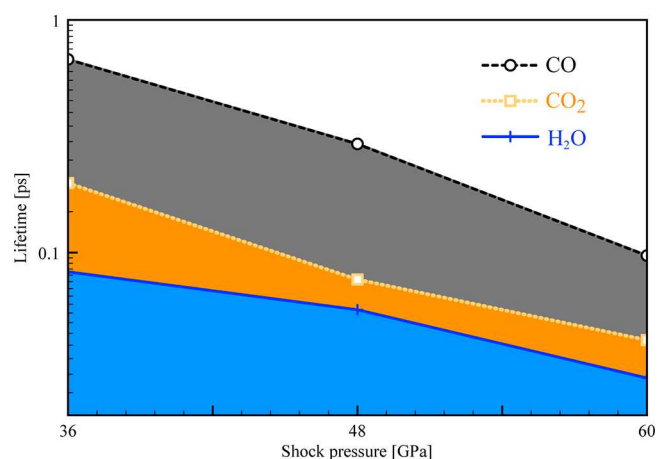
Shock compression simulations were conducted using the well-established multiscale shock compression simulation technique (MSST).<sup>28,29,52</sup> MSST operates by time-evolving equations of motion for the atoms and for the atoms and computational cell dimension in the direction of the shock to constrain the stress in the propagation direction to the Rayleigh line and the energy of the system to the Hugoniot energy condition.<sup>52,53</sup> (The Hugoniot is the locus of thermodynamic end states achieved by a specific shock velocity and set of initial conditions.) For a given shock speed, these two relations describe a steady planar shock wave within continuum theory. MSST has been used in conjunction with quantum simulation methods to accurately reproduce the shock Hugoniot of a number of systems.<sup>29–31,34,41,54–56</sup> New MSST equations of motion used in this study allow for a self-consistent dynamic electron temperature, where the ionic and electronic temper-

atures are kept equal at all times.<sup>57</sup> This can result in a lowering of the Hugoniot end states in the shock compressed material due to the heat capacity of the electrons, which is nonzero when thermal electronic excitations are present.<sup>57,58</sup> At shock velocities of 9 and 10 km/s, we used a scaling term with the MSST ionic equations of motion to account for drift in the conserved quantity in our simulations.<sup>32,56</sup> A scaling factor of  $10^{-3}$  resulted in a deviation in the total forces in our simulations of less than 1% once a steady shock compression had been produced. We allowed the system to evolve for up to 100 ps within the shock state. The deviation from the Hugoniot energy and Rayleigh line conditions for all of our shock compression simulations was less than 1%.

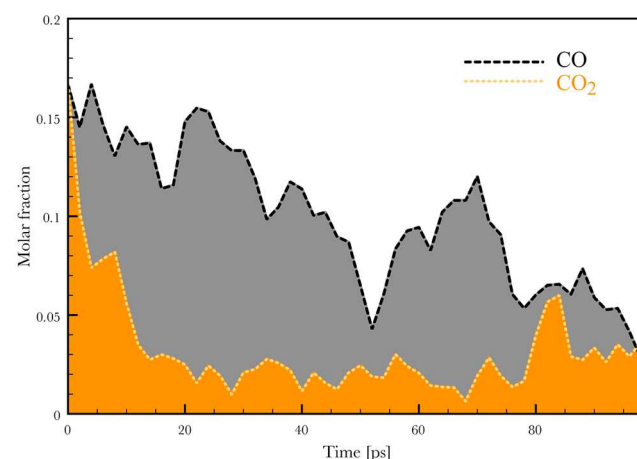
Adiabatic expansion simulations were conducted using the DOLLS algorithm,<sup>59</sup> where the simulation cell was expanded at a constant rate until the initial density of  $1.0 \text{ g/cm}^3$  was achieved. The rate of expansion was varied by an order of magnitude, i.e.,  $k_x^{-1} = 10\text{--}100 \text{ ps}$ . We found that chemical reactivity in these simulations was consistent with values of  $k_x^{-1} \geq 50 \text{ ps}$ . Hence, our chemical analysis discusses results from our 50 ps expansions, only. After the expansion, the system was cooled to 300 K using a temperature ramp for approximately 20 ps, followed by equilibration at 300 K using Nose–Hoover thermostat chains for up to an additional 20 ps. Calculations corresponding to the longest expansion rate had a total simulation time (regions I, II, and III) of approximately 260 ps and encompassed a wide range of different thermodynamic conditions (Figure 1). The time frame on which a comet impact occurs is on the order of seconds,<sup>34</sup> which is well beyond the means of molecular dynamics simulations. However, our simulations reported here describe processes and dynamics on a time scale an order of magnitude larger than the rise-time of shocks in polycrystalline materials,<sup>19–21,60,61</sup> shock compressed water,<sup>30</sup> and our previous DFT-MD results.<sup>34</sup> Our impact simulations thus span the relevant time scales corresponding to the initial chemistry within an ice grain in a comet. These time scales are amenable to study by laser shock compression experiments.<sup>20,60,61</sup>

## RESULTS AND DISCUSSION

Our initial icy mixture was subject to shock velocities of 5–10 km/s, which yielded Hugoniot pressures from 11 to 60 GPa and temperatures from 974 to 4600 K (Figure 2). The particle velocity  $U_p$  from our shock compression simulations was taken to be equal to the impact velocity<sup>34</sup> and is related to the angle from the horizon  $\varphi$  according to the formula:  $U_p = (V_E/2) \sin \varphi$ . Here,  $U_p$  is computed according to the relation  $U_p = U_s(1 - \rho_0/\rho)$ , where  $U_s$  is the shock velocity imparted to the system,  $\rho_0$  is the density of the initial preshock state, and  $V_E$  is the encounter velocity of the impacting extraterrestrial icy object. Impact with an ocean or other body with similar shock impedance to the extraterrestrial ice contributes an approximate factor of 1/2 due to the body's compressibility. An astrophysical ice with initial velocity of 29 km/s (approximate median encounter velocity of a short period comet with Earth<sup>17</sup>) would have to impact the Earth at an angle from the horizontal of up to  $25^\circ$  to experience the pressures and temperatures of our simulations. Assuming a probability distribution of  $dP = \sin(2\varphi) d\varphi$ , where  $\varphi$  is the angle from the horizon,<sup>62</sup> our simulations correspond to low velocity impacts with a cumulative 18% probability. Thus, our study encompasses likely events for astrophysical ice impacts on early Earth.



(a) CO, CO<sub>2</sub> and H<sub>2</sub>O lifetimes



(b) CO and CO<sub>2</sub> concentrations

**Figure 4.** (a) Lifetimes of H<sub>2</sub>O, CO, and CO<sub>2</sub> under increasingly stronger shocks. At 36 GPa, CO has a lifetime close to 1 ps, whereas CO<sub>2</sub> and H<sub>2</sub>O have lifetimes closer to 0.1 ps. At 60 GPa, all three species have lifetimes of 0.1 ps or less. (b) CO and CO<sub>2</sub> concentration vs time in the 36 GPa shock (region I). CO is less reactive than CO<sub>2</sub> and subsequently its concentration achieves a steady state over significantly longer time scales.

We note a softening of the  $P$ – $\rho$  Hugoniot curve from DFTB (Figure 2a) between  $2.07 \text{ g/cm}^3$  (7 km/s, 25 GPa) and  $2.27 \text{ g/cm}^3$  (8 km/s, 36 GPa), which we attribute to the onset of chemical decomposition of the starting materials and the formation of C–C and C–N bonds (discussed below). As a result, we have focused our discussion on simulations of shock velocities of 8 km/s (36 GPa, 2700 K), 9 km/s (48 GPa, 3700 K), and 10 km/s (60 GPa, 4600 K). Our DFTB simulations yielded Hugoniot curves that deviate up to 13% in pressure and 38% in temperature from results from DFT<sup>34</sup> (Figure 2). However, at shock velocities between 8 and 10 km/s, the deviations from DFT are 3–5% in pressure and 13–19% in temperature. A constant pressure–temperature state was achieved in all of our shock compression simulations within 5 ps (Figure 1). We observed the creation of new C–C and C–N bonds during this steady state, where the beginnings of carbon and nitrogen containing rings could be observed, and little of the starting material remains. Expansion to the initial density yielded a high-temperature state where C–C and C–N chemistry had largely been quenched. Equilibration simulations

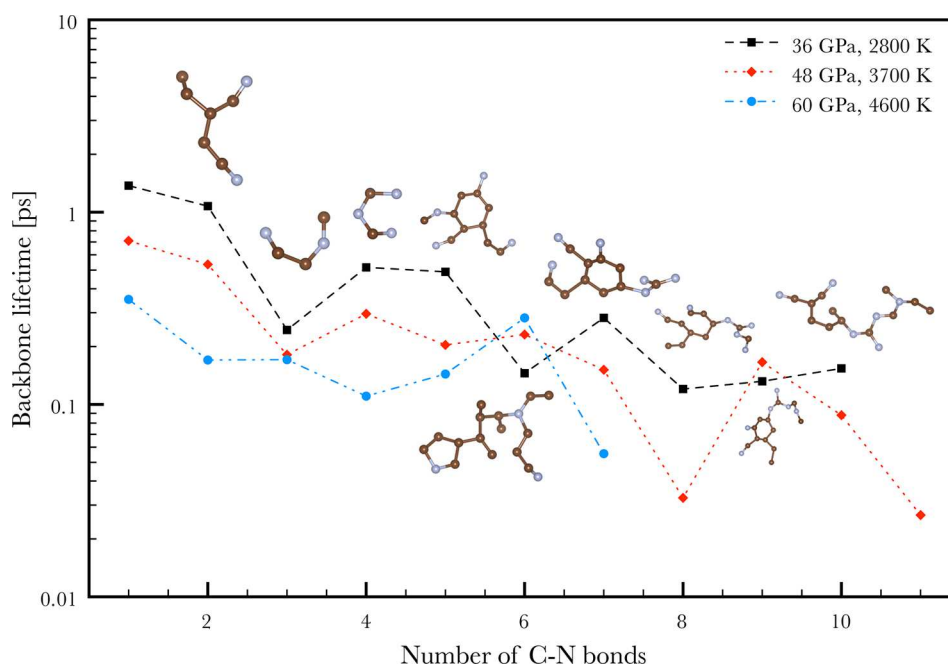


**Figure 5.** C–N bonded backbones produced during shock compression simulation as a function of the number of C–N bonds. Inset graphics correspond to backbone structures produced during the 36 GPa compression. Here, brown circles correspond to carbon and blue to nitrogen.

then yielded a variety of new, stable C–C and C–N bonded compounds.

Analysis of the time evolution of the radial distribution functions (RDFs), viz.,  $g(r) = V/N^2 \langle \sum_{i,j} \delta(r-r_{ij}) \rangle$ , provides a general picture for the different types of new bonds that can occur during impact events. For shock conditions of 36 GPa and 2800 K (Figure 3), we observe that compression induces the formation of a new C–C covalent bond peak centered at slightly less than 1.5 Å, consistent with graphite and diamond nearest neighbor distances of  $\sim 1.42$  and 1.55 Å, respectively.<sup>55,56</sup> In addition, we observe the appearance of two new overlapping C–N covalent bond peaks between 1.0 and 1.5 Å consistent with different bond orders, such as triple bonds (e.g., HCN) and single bonds (e.g., amino acids). During adiabatic expansion, the C–C bond peak has shifted to slightly higher distance due to the lower pressures attained. In addition, the C–N bond peaks have further separated, and appear more distinct. Chemical reactivity appears to be largely quenched by 15 GPa and 2300 K, and the only reactions we observe are reversible proton exchange. During the cooling and equilibration step, we observe broad C–C bond peaks between 1.2–1.55 Å, corresponding to differing degrees of *sp* hybridization. There are a number of C–N bond peaks, including one at  $\sim 1.1$  Å one at  $\sim 1.3$  Å and one at  $\sim 1.4$  Å. These can correspond to nitrile (e.g., R–CN), amide (e.g., R–CO–NH<sub>2</sub>), and amine functional groups (e.g., R–CH<sub>2</sub>–NH<sub>2</sub>), respectively.

We now determine the specific chemical reactivity in our simulations using a pre-established methodology of optimal bond cutoff distances and lifetimes.<sup>26,27,34,63</sup> We define molecular species by first choosing an optimal bonding cutoff  $r_c$  for all possible bonds. The optimal value for  $r_c$  to distinguish between bonded and nonbonded atomic sites is given by the first minimum in the corresponding pair radial distribution function  $g(r)$ , which corresponds to the maximum of the potential of mean force, viz.,  $W(r) = -k_B T \ln[g(r)]$ , for all possible bonding pairs. This choice corresponds to the optimal definition of the transition state within transition state theory.<sup>63</sup>

In addition, to avoid counting species that were entirely transient and not chemically bonded,<sup>26</sup> we also chose a lifetime cutoff  $\tau_c$  of 20 fs for O–H and C–H bonds and 50 fs for all other (N.B., no H–H bonds were detected in any of our simulations). This criteria is intuitive because bonds with this lifetime could conceivably be detected spectroscopically. As a result, atom pairs were considered to be bonded only if they resided within a distance of each other of  $r_c$  for a time of greater than  $\tau_c$ . Using these bonding criteria, specific molecular species were then defined by recursively creating a data tree of all atomic bonds branching from the original bonded pair. The chemical reactivity, concentrations, and lifetimes of different species were then determined by monitoring the creation and dissociation of specific molecules during the course of the simulations. Shorter and longer bond-lifetime criteria were also tested. We found that the computed species at quenched conditions and overall conclusions of this work were independent of these parameters. The concentrations of species at high pressure and temperature have some dependence on bond and lifetime criteria, as expected and has been shown for other hot dense materials.<sup>30,34,63</sup>

We observe that the sudden increase in pressure and temperature due to shock loading causes the starting materials to become highly reactive (Figure 4a). In particular, H<sub>2</sub>O has a computed lifetime of less than 0.1 ps at a shock pressure of 36 GPa and decreases to a value of approximately 20 fs at 60 GPa, similar to previous DFT-MD results.<sup>30,34</sup> This is many orders of magnitude shorter than its lifetime at ambient conditions ( $\sim 10$  h<sup>64</sup>). We find that CO has a significantly higher lifetime than CO<sub>2</sub> under these dissociative conditions, with a value close to 1 ps at 36 GPa, compared to slightly over 0.1 ps for CO<sub>2</sub> at the same conditions. At 60 GPa, the CO lifetime has decreased to  $\sim 0.1$  ps, compared to 0.05 ps for CO<sub>2</sub>. Similar chemical properties were observed in our original DFT-MD simulations, such as the kinetics of starting material decomposition and CO having a longer lifetime than CO<sub>2</sub> at lower shock pressures. At 36 GPa, CO exhibits long time-scale reactivity, where its

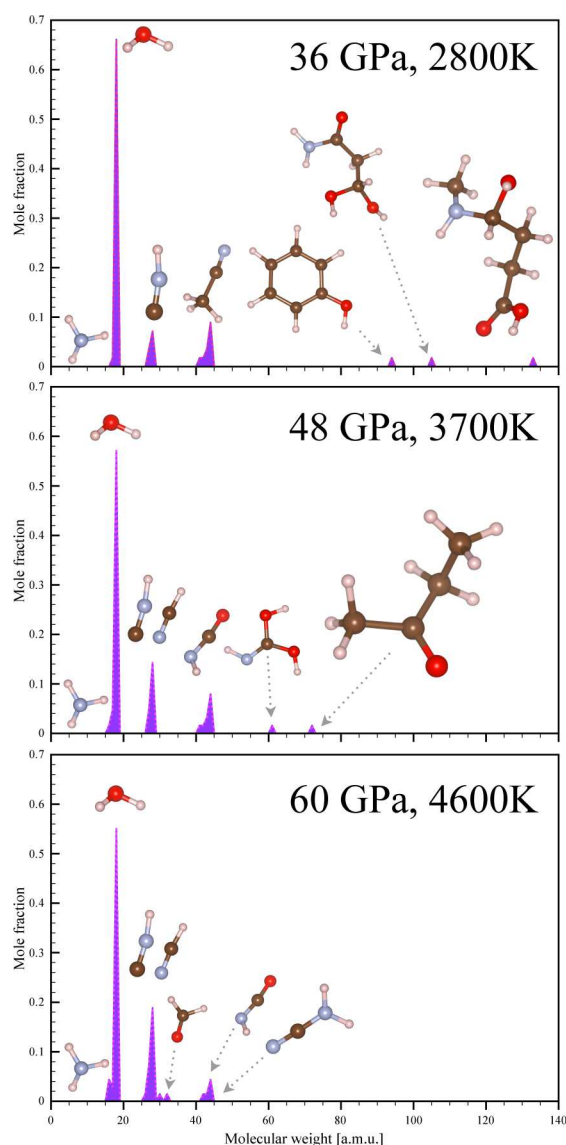


**Figure 6.** Simulated mass spectra for expansion products from different shock states. Brown circles correspond to carbon, blue to nitrogen, red to oxygen, and white to hydrogen. All data shown correspond to an expansion rate of  $k_x = 50 \text{ ps}^{-1}$  in region II. Shock compression 36 GPa tended to yield final products with greater chemical complexity, whereas shock compression to 48 and 60 GPa yielded a variety of smaller molecules relevant to prebiotic synthesis.

concentration has not achieved a steady state over the 100 ps duration of our shock compression simulation (Figure 4b). In contrast,  $\text{CO}_2$  concentrations achieve a steady state within 20 ps. The heightened reactivity of  $\text{CO}_2$  could be due to the presence of an ionic phase, observed experimentally at similar conditions.<sup>65</sup> Here, the C–O bonds can be weakened due to mixed covalent/ionic character,<sup>63</sup> which in turn promotes reactivity. At shock conditions of 46 and 60 GPa, we observe that the concentrations of all starting materials achieved a steady state within 20 ps.

The reactive thermodynamic conditions studied here yield a large number of different C–C and C–N bonded oligomers, with lifetimes generally less than 0.05 ps. However, these oligomers tend to be composed of a series of longer-lived C–C and C–N bonded backbones that can have lifetimes on the order of 1 ps (Figure 5), with smaller moieties such as hydroxyl

groups diffusing on and off the backbones at rapid rates. Conditions of 36 GPa and 2800 K appear to reside in a “sweet-spot” for complexity in shock synthesis, where we observe a variety of C–C and C–N bonded backbones with lifetimes greater than 0.1 ps. Several C–N backbones containing a six-member carbon ring were produced, with empirical formulas of  $\text{C}_{10}\text{N}_4$ ,  $\text{C}_{10}\text{N}_6$ , and  $\text{C}_{12}\text{N}_6$ . In addition, a backbone with the formula  $\text{C}_{15}\text{N}_3$  exhibited a five-member nitrogen containing heterocycle. Graphite-like sheets containing nitrogen-rich heterocycles have been reported in simulations of organic energetic materials at similar conditions.<sup>33</sup> A shock pressure of 36 GPa also produced a small number of linear backbones containing C–C bonds only, with 2–7 carbon atoms. Shock conditions of 48 GPa and 3700 K, and 60 GPa and 4600 K produced a wide distribution of simpler C–C and C–N bonded backbones which tend to be more chain-like, and have shorter lifetimes due to the higher thermodynamic conditions.

Expansion and cooling to ambient conditions causes the C–C and C–N bonded backbones mainly to dissociate and form a number of stable, new compounds (Figure 6). The same proteinogenic glycine derivatives as in our previous study were not found,<sup>34</sup> though our current study did yield a number of highly relevant prebiotic precursors. All of our expansion simulations recovered significant amounts of water and  $\text{NH}_3$ , and yielded relatively large concentrations of HCN and HNC. These products could yield amino acids, pyrimidines, and/or purines in aqueous solution.<sup>3,8,66</sup> HCN/HNC can be hydrolyzed to form formaldehyde and ammonia.<sup>67</sup> Formaldehyde can react with cyano groups and  $\text{NH}_3$  to form amino acids via Strecker synthesis.<sup>8</sup> Liquid HCN is known to polymerize spontaneously in the presence of a base, such as an amine or ammonia, or in aqueous solution. Cleavage products of these polymers include  $\alpha$ -amino acids, purines, pyrimidines, and polypeptides.<sup>68</sup> Expansion from shock conditions of 36 GPa produced functionalized aromatic hydrocarbons, including the six-member carbon ring containing compound phenol (e.g., benzene plus a hydroxyl group). Benzene chemistry is the first step in the formation of polycyclic aromatic hydrocarbons (PAHs), fullerene-type materials, and could be a prebiotic precursor for nucleotides of RNA and DNA.<sup>69</sup> We note the formation of a propyl carboxamide containing a diol substituent at these conditions. At equilibrium time scales, this would likely decompose into  $\beta$ -alanine, a naturally occurring  $\beta$ -amino acid. We also observe the formation of a  $\gamma$  secondary amino acid with a four-member carbon chain at a molecular mass of 130 amu, chemically similar to the mammalian neurotransmitter  $\gamma$ -aminobutyric acid.

Expansion from shock conditions of 48 and 60 GPa produced measurable concentrations of  $\text{CH}_4$  and isocyanic acid (HNCO). Isocyanic acid reacts with amines ( $\text{R-NH}_2$ ) to form ureas (e.g., nucleobase precursors) through carbamylation. Cyanuric acid (i.e., isocyanic acid trimer) has been shown experimentally to yield heterocycles of increasing complexity and biological potential at similar thermodynamic conditions to our study.<sup>70</sup> At a shock pressure of 48 GPa, an amine-diol is synthesized at a molecular mass of 49 amu that is likely to decompose into formamide on equilibrium time scales. Formamide is unstable at standard pressures and temperatures but can react with itself to form purine in the form of the nucleic acid base pair adenine.<sup>71</sup> We also note the presence of methyl propyl ketone (2-pentanone) at 72 amu. Shock conditions of 60 GPa yielded both formaldehyde and cyanamide. In aqueous solution, cyanamide forms the dimer

dicyandiamide, which is active in forming peptides.<sup>72</sup> The larger relative amounts of NH<sub>3</sub> and HCN/HNC at these conditions could enhance Strecker amino acid synthesis due to stronger impacts such as these on planetary surfaces.

## CONCLUSIONS

Our results provide a mechanism for shock synthesis of a wide variety of prebiotic molecules at realistic impact conditions that is independent of external features or the specific chemical environment on a planet. All of the reactive conditions studied here yielded significant quantities of HCN, HNC, HNCO, and other simple precursors for more complex organic molecules. Impact events with shock conditions of 36 GPa and 2800 K yielded compounds with a relatively high degree of complexity, including phenol and precursors to  $\beta$  and  $\gamma$  amino acids. An intermediate impact event with shock conditions of 48 GPa and 3700 K yielded a smaller degree of complexity, though it did produce some longer-chain carbon containing compounds, and a variety of simpler molecules that are likely important for terrestrial amino acid synthesis. Finally, the highest shock conditions studies here of 60 GPa and 4600 K yielded a wide variety of simpler compounds that are precursors to amino acids and peptides. The enhanced formation of species such as formaldehyde and cyanamide could indicate that stronger, more direct impact of cometary material with early Earth could have yielded important precursors for more complex prebiotic synthesis. Our results provide a mechanism for the shock synthesis of prebiotic materials on extra-terrestrial environments as well, such as Saturn's satellite Titan, which is known to have a dense, hydrocarbon containing atmosphere.<sup>73,74</sup> Complete knowledge of the chemical properties of prebiotic mixtures under extreme thermodynamic conditions is needed to understand the role of impact events in the formation of life-building compounds both on early Earth and on other planets.

## AUTHOR INFORMATION

### Corresponding Author

\*E-mail: ngoldman@llnl.gov.

### Notes

The authors declare no competing financial interest.

## ACKNOWLEDGMENTS

The authors thank Lukasz Koziol for a critical reading of the manuscript, and Liam Krauss for creation of the graphical TOC image. This work was performed under the auspices of the U.S. Department of Energy by Lawrence Livermore National Laboratory under Contract DE-AC52-07NA27344 and was funded by the National Aeronautics and Space Administration (NASA), Astrobiology: Exobiology and Evolutionary Biology program (#NNH11AQ671). Computations were performed at LLNL using the Aztec and RZCereal massively parallel computers.

## REFERENCES

- (1) Miller, S. L. *Science* **1953**, *117*, 528.
- (2) Miller, S. L.; Urey, H. C. *Science* **1959**, *130*, 245.
- (3) Engel, M. H. *Pre-biotic organic synthesis: Laboratory simulation experiments and their significance for the origin of life in the solar system*. 2011; Conference on Instruments, Methods, and Missions for Astrobiology XIV, San Diego, CA, Aug 23–25, 2011.
- (4) Harada, K.; Fox, S. *Nature* **1964**, *201*, 335–336.
- (5) LaRowe, D.; Regnier, P. *Origins of Life and Evolution of the Biosphere* **2008**, *38*, 383–397.

- (6) Sagan, C.; Khare, B. N. *Science* **1971**, *173*, 417–420.
- (7) Bernstein, M. P.; Dworkin, J. P.; Sandford, S. A.; Cooper, G. W.; Allamandola, L. J. *Nature* **2002**, *416*, 401.
- (8) Brack, A. *Chem. Biodiversity* **2007**, *4*, 665.
- (9) Bar-Nun, A.; Bar-Nun, N.; Bauer, S. H.; Sagan, C. *Science* **1970**, *168*, 470.
- (10) McKay, C. P.; Borucki, W. J. *Science* **1997**, *276*, 390.
- (11) B. Fegley, J.; Prinn, R. G.; Hartman, H.; Watkins, G. H. *Nature* **1986**, *319*, 305.
- (12) Chyba, C. F.; Thomas, P. J.; Brookshaw, L.; Sagan, C. *Science* **1990**, *249*, 366.
- (13) Ehrenfreund, P.; Irvine, W.; Becker, L.; Blank, J.; Brucato, J. R.; Colangeli, L.; Derenne, S.; Despois, D.; Dutrey, A.; Fraaije, H.; Lazcano, A.; Owen, T.; Robert, F. An International Space Science Institute ISSI-Team. *Rep. Prog. Phys.* **2002**, *65*, 1427.
- (14) Ehrenfreund, P.; Charnley, S. B. *Annu. Rev. Astron. Astrophys.* **2000**, *38*, 427.
- (15) Elsila, J. E.; Glavin, D. P.; Dworkin, J. P. *Meteorit. Planet. Sci.* **2009**, *44*, 1323.
- (16) Muñoz Caro, G. M.; Meierhenrich, U. J.; Schute, W. A.; Barbier, B.; Arcones Segovia, A.; Rosenbauer, H.; Thiemann, W. H.-P.; Brack, A.; Greenberg, J. M. *Nature* **2002**, *416*, 403.
- (17) Blank, J. G.; Miller, G. H.; Ahrens, M. J.; Winans, R. E. *Origins Life Evol. Biospheres* **2001**, *31*, 15.
- (18) Meech, K. J.; Hainaut, O. R.; Marsden, B. G. *Icarus* **2004**, *170*, 463.
- (19) Robertson, D. H.; Brenner, D. W.; White, C. T. *Phys. Rev. Lett.* **1991**, *67*, 3132.
- (20) Gahagan, K. T.; Moore, D. S.; Funk, D. J.; Rabie, R. L.; Buelow, S. J. *Phys. Rev. Lett.* **2000**, *85*, 3205.
- (21) Kadau, K.; Germann, T. C.; Lomdhal, P. S.; Holian, B. L. *Science* **2002**, *296*, 1681.
- (22) Furukawa, Y.; Sekine, T.; Oba, M.; Kakegawa, T.; Nakazawa, H. *Nat. Geosci.* **2009**, *2*, 62.
- (23) Kress, J. D.; Mazevet, S.; Collins, L. A.; Wood, W. W. *Phys. Rev. B* **2000**, *63*, 024203.
- (24) Gygi, F.; Galli, G. *Phys. Rev. B* **2002**, *65*, 220102.
- (25) Correa, A. A.; Bonev, S. A.; Galli, G. *Proc. Natl. Acad. Sci. U. S. A.* **2006**, *103*, 1204.
- (26) Goldman, N.; Fried, L. E. *J. Chem. Phys.* **2006**, *125*, 044501.
- (27) Goldman, N.; Fried, L. E. *J. Chem. Phys.* **2007**, *126*, 134505.
- (28) Reed, E. J.; Manaa, M. R.; Fried, L. E.; Glaesemann, K. R.; Joannopoulos, J. D. *Nat. Phys.* **2008**, *4*, 72–76.
- (29) Mundy, C. J.; Curioni, A.; Goldman, N.; Kuo, I.-F.; Reed, E.; Fried, L. E.; Ianuzzi, M. *J. Chem. Phys.* **2008**, *128*, 184701.
- (30) Goldman, N.; Reed, E. J.; Kuo, I.-F. W.; Fried, L. E.; Mundy, C. J.; Curioni, A. *J. Chem. Phys.* **2009**, *130*, 124517.
- (31) Goldman, N.; Reed, E. J.; Fried, L. E. *J. Chem. Phys.* **2009**, *131*, 204103.
- (32) Reed, E. J.; Maiti, A.; Fried, L. E. *Phys. Rev. E* **2009**, *81*, 016607.
- (33) Manaa, M. R.; Reed, E. J.; Fried, L. E.; Goldman, N. *J. Am. Chem. Soc.* **2009**, *131*, 5493.
- (34) Goldman, N.; Reed, E. J.; Fried, L. E.; Kuo, I.-F. W.; Maiti, A. *Nat. Chem.* **2010**, *2*, 949.
- (35) Martins, Z.; Price, M. C.; Goldman, N.; Sephton, M. A.; Burchell, M. J. *Nat. Geosci.* **2012**, submitted.
- (36) Aradi, B.; Hourahine, B.; Frauenheim, T. *J. Phys. Chem. A* **2007**, *111*, 5678 <http://www.dftb-plus.info>.
- (37) Elstner, M.; Porezag, D.; Jungnickel, G.; Elsner, J.; Haugk, M.; Frauenheim, T.; Suhai, S.; Seifert, G. *Phys. Rev. B* **1998**, *58*, 7260.
- (38) Manaa, M. R.; Fried, L. E.; Melius, C. F.; Elstner, M.; Frauenheim, T. *J. Phys. Chem. A* **2002**, *106*, 9024.
- (39) Margetis, D.; Kaxiras, E.; Elstner, M.; Frauenheim, T.; Manaa, M. R. *J. Chem. Phys.* **2002**, *117*, 788.
- (40) Manaa, M. R.; Reed, E. J.; Fried, L. E.; Galli, G.; Gygi, F. *J. Chem. Phys.* **2004**, *120*, 10146.
- (41) Qi, T.; Reed, E. J. *J. Phys. Chem. A* **2012**, *116*, 10451–10459.
- (42) Plimpton, S. J. *Comput. Phys.* **1995**, *117*, 1 <http://lammps.sandia.gov>.

- (43) Niklasson, A. M. N.; Tymczak, C. J.; Challacombe, M. *Phys. Rev. Lett.* **2006**, *97*, 123001.
- (44) Niklasson, A. M. N. *Phys. Rev. Lett.* **2008**, *100*, 123004.
- (45) Niklasson, A. M. N.; Steneteg, P.; Odell, A.; Bock, N.; Challacombe, M.; Tymczak, C. J.; Holmström, E.; Zheng, G.; Weber, V. *J. Chem. Phys.* **2009**, *130*, 214109.
- (46) Odell, A.; Delin, A.; Johansson, B.; Bock, N.; Challacombe, M.; Niklasson, A. M. N. *J. Chem. Phys.* **2010**, *131*, 244106.
- (47) Zheng, G.; Niklasson, A. M. N.; Karplus, M. *J. Chem. Phys.* **2011**, *135*, 044122.
- (48) Sanville, E. J.; Bock, N.; Niklasson, A. M. N.; Cawkwell, M. J.; Sewell, T. D.; Dattelbaum, D. M.; Sheffield, S. A. *Proceedings of the 14th International Symposium on Detonation*; Office of Naval Research: Washington, DC, 2011; p 91.
- (49) Mermin, N. D. *Phys. Rev.* **1965**, *137*, 1441.
- (50) Nosé, S. *Mol. Phys.* **1984**, *52*, 255.
- (51) Hoover, W. G. *Phys. Rev. A* **1985**, *31*, 1695.
- (52) Reed, E. J.; Fried, L. E.; Joannopoulos, J. D. *Phys. Rev. Lett.* **2003**, *90*, 235503.
- (53) Reed, E. J.; Fried, L. E.; Henshaw, W. D.; Tarver, C. M. *Phys. Rev. E* **2006**, *74*, 056706.
- (54) Wu, C.; Fried, L. E.; Yang, L. H.; Goldman, N.; Bastea, S. *Nat. Chem.* **2009**, *1*, 57.
- (55) Goldman, N.; Fried, L. E. *J. Phys. Chem. C* **2012**, *116*, 2198.
- (56) Goldman, N.; Srinivasan, S. G.; Hamel, S.; Fried, L. E.; Gaus, M.; Elstner, M. *J. Phys. Chem. C* **2013**, <http://dx.doi.org/10.1021/jp312759j>.
- (57) Reed, E. J. *J. Phys. Chem. C* **2012**, *116*, 2205.
- (58) Mattsson, T. R.; Desjarlais, M. P. *Phys. Rev. Lett.* **2006**, *97*, 017801.
- (59) Hoover, W. G.; Evans, D. J.; Hickman, R. B.; Ladd, A. J. C.; Ashurst, W. T.; Moran, B. *Phys. Rev. A* **1980**, *22*, 1690.
- (60) Armstrong, M. R.; Crowhurst, J. C.; Bastea, S.; Zaug, J. M. *J. Appl. Phys.* **2010**, *108*, 023511.
- (61) Crowhurst, J. C.; Armstrong, M. R.; Knight, K. B.; Zaug, J. M.; Behymer, E. M. *Phys. Rev. Lett.* **2011**, *107*, 144302.
- (62) Shoemaker, E. M. In *The Physics and Astronomy of the Moon*; Kopal, Z., Ed.; Academic Press: New York, 1962; pp 283–359.
- (63) Goldman, N.; Fried, L. E.; Kuo, I.-F. W.; Mundy, C. J. *Phys. Rev. Lett.* **2005**, *94*, 217801.
- (64) Geissler, P. L.; Dellago, C. D.; Chandler, D.; Hutter, J.; Parrinello, M. *Science* **2001**, *291*, 2121–2124.
- (65) Yoo, C.-S.; Sengupta, A.; Kim, M. *Angew. Chem., Int. Ed.* **2011**, *50*, 11219–11222.
- (66) Miller, S. L. *Ann. N. Y. Acad. Sci.* **1957**, *69*, 260–275.
- (67) Danger, G.; Plasson, R.; Pascal, R. *Chem. Soc. Rev.* **2012**, *41*, 5416–5429.
- (68) Matthews, C. N.; Minard, R. D. *Faraday Discuss.* **2006**, *133*, 393–401.
- (69) Ehrenfreund, P.; Rasmussen, S.; Cleaves, J.; Chen, L. *Astrobiology* **2006**, *6*, 490–520.
- (70) Montgomery, W.; Crowhurst, J. C.; Zaug, J. M.; Jeanloz, R. J. *Phys. Chem. B* **2008**, *112*, 2644–2648.
- (71) Wang, J.; Gu, J.; Nguyen, M. T.; Springsteen, G.; Leszczynski, J. *J. Phys. Chem. B* **2013**, *117*, 2314–2320.
- (72) Brack, A., Ed. *The Molecular Origins of Life: Assembling Pieces of the Puzzle*; Cambridge University Press: Cambridge, U.K., 1998.
- (73) Raulin, F.; Brasse, C.; Poch, O.; Coll, P. *Chem. Soc. Rev.* **2012**, *41*, 5380–5393.
- (74) Kaiser, R. I.; Mebel, A. M. *Chem. Soc. Rev.* **2012**, *41*, 5490–5501.